Supplementary information for the manuscript:

Monitoring and engineering reactor microbiomes of denitrifying bioelectrochemical systems

Authors: N. Pous, C. Koch, A. Vilà-Rovira, M.D. Balaguer, J. Colprim, J. Mühlenberg, S. Müller, F. Harnisch, F. and S. Puig.

Summary:

Video 1. Evolution of cytometric measurements at the four sampling ports: SP-A (green), SP-B (violet), SP-C (blue) and SP-D (orange).

S1: Analyses of N_2O using gas chromatography.

Instrumental:

The analyses of N_2O were performed on an Agilent 7890A GC/µECD system with an Agilent G1888 headspace autosampler.

Gas chromatograph

The injection mode was split 1:10. The injector temperature was kept at 250 °C. For the separation a HP-Plot/Q column (30 m x 0.53 mm x 40 µm; Agilent Technologies) was used. The gas chromatography system was operating at programmed-temperature-mode as follows: initial temperature 40 °C hold for 4 min, linear ramp 30 °C·min^{-1} till 220 °C and hold for 1 min. A µECD (electron capture detector) heated at 250 °C was used for data acquisition.

Headspace-sampler

Table S1. Instrumental settings of the headspace-sampler.

Temperatures		**Timing**		**Pressures**	
Oven	90 °C	Vial equilibration	0.5 min	Carrier	7.0 psi
Loop (1 ml)	150 °C	Pressurization	0.5 min	Vial	7.2 psi
Transfer line	180 °C	Loop fill	0.4 min		
		Loop equilibration	0.1 min		
		Inject	0.4 min		

Sample preparation:

For the analysis 3 mL of sample were placed in a 20-mL headspace vial and tightly closed with an aluminium crimp cap with PTFE/silicone septum using a hand crimper. Samples have to be carefully transferred from experimental equipment to the 20 mL vial, to prevent loss of nitrous oxide by shaking or outgassing.

Calibration was done by analyzing different dilutions of a saturated N_2O-solution. Water has been filled into a 100 mL volumetric flask and the nitrous oxide was passed through a filter with 300 mL·min^{-1} for 3 min at room temperature and atmospheric pressure. The solubility of nitrous oxide at 20 °C and atmospheric pressure is 1200 mg·L^{-1}.[1] Calibration levels were between 2.4 and 600 mg·L^{-1}. The detection limit is 2.4 mgL^{-1} .

S2: Computational fluid dynamics calculation

The velocities generated inside the cathode were calculated using a computational fluid dynamics program (Ansys Fluent v12.1 [2]). To do this, both mass and momentum equations were solved. The mass conservation is shown in equation S1.

$$\frac{d\rho}{dt} + \nabla\cdot(\rho\vec{v}) = S_m \quad \text{(eq. S1)}$$

Where ρ is the fluid density, *v* represents the velocity vector, and S_m is a source term (by chemical reaction, phases mass exchanges, among others).

The equation of momentum conservation in an inertial (non-accelerating) reference frame is described as shown in equation S2.

$$\frac{d}{dt}(\rho\vec{v}) + \nabla\cdot(\rho\vec{v}\vec{v}) = -\nabla p + \nabla\cdot(\bar{\tau}) + \rho\vec{g} + \vec{F} \quad \text{(eq. S2)}$$

From which ρ is the static pressure, ρg and F are gravitational and external body forces, and τ is the stress tensor, which is calculated using equation S3.

$$\vec{\tau} = \mu\left[\left(\nabla\vec{v} + \nabla\vec{v}^T\right) - \frac{2}{3}\nabla\cdot\vec{v}I\right] \quad \text{(eq. S3)}$$

Steady state simulations were developed considering single water based phase. To close the solution of the different solutions, velocity inlet boundary conditions for the influent/outflow streams, as well as for both recirculation streams were defined, taking in account the fluxes specified in experimental section. The inlet recirculation streams values were formulated based on the values from the outflow recirculation stream. Wall boundary conditions were developed for the methacrylate walls of the reactor as well as for the rod graphite surface. The simulations were performed at a constant temperature of 22ºC and atmospheric pressure. The influent flow and the recirculation loop generated heterogeneous flows inside this chamber, which suggested zones with different nitrate availability.

S3: Gate template used for flow cytometry data analyses.

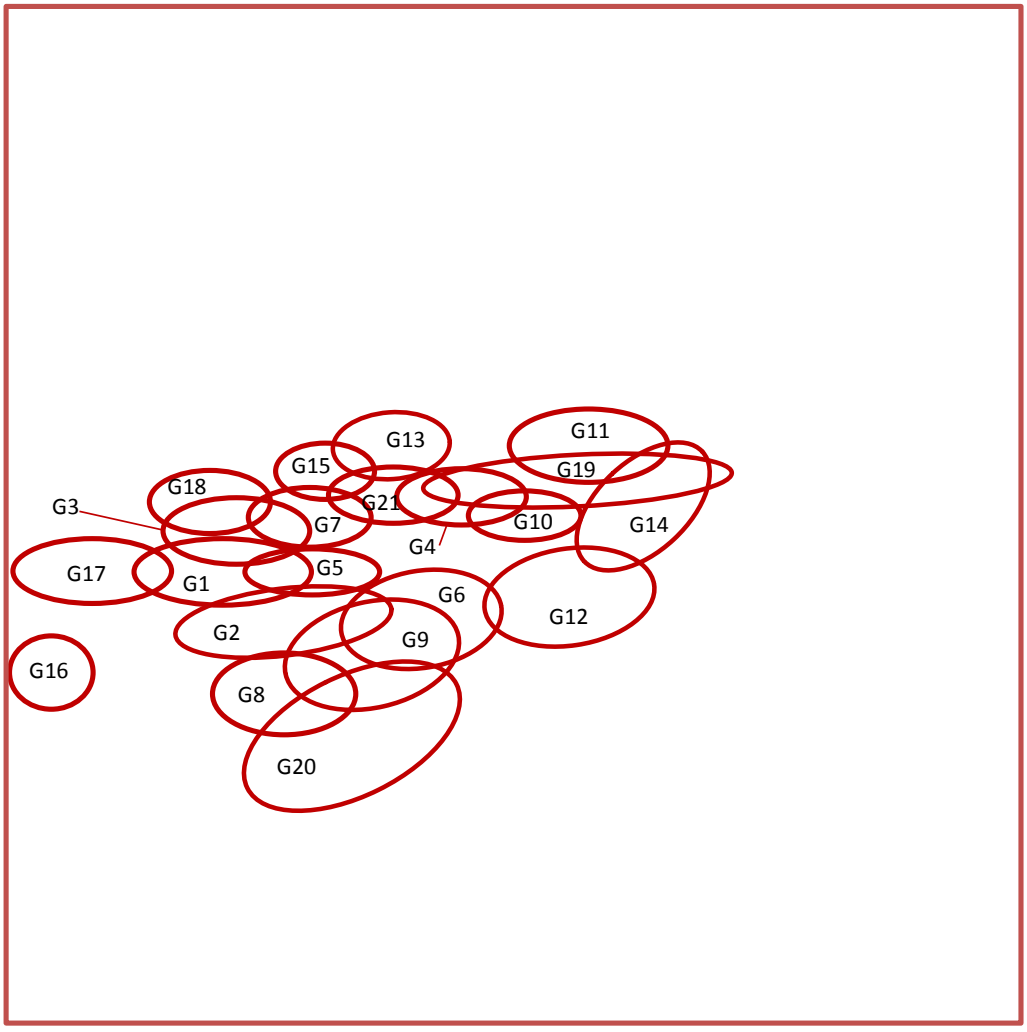

Figure S1. Gate template used for flow cytometry data analyses.

S4: Absolute current density and nitrate, nitrite and nitrous oxide consumption rates at the different stress-tests.

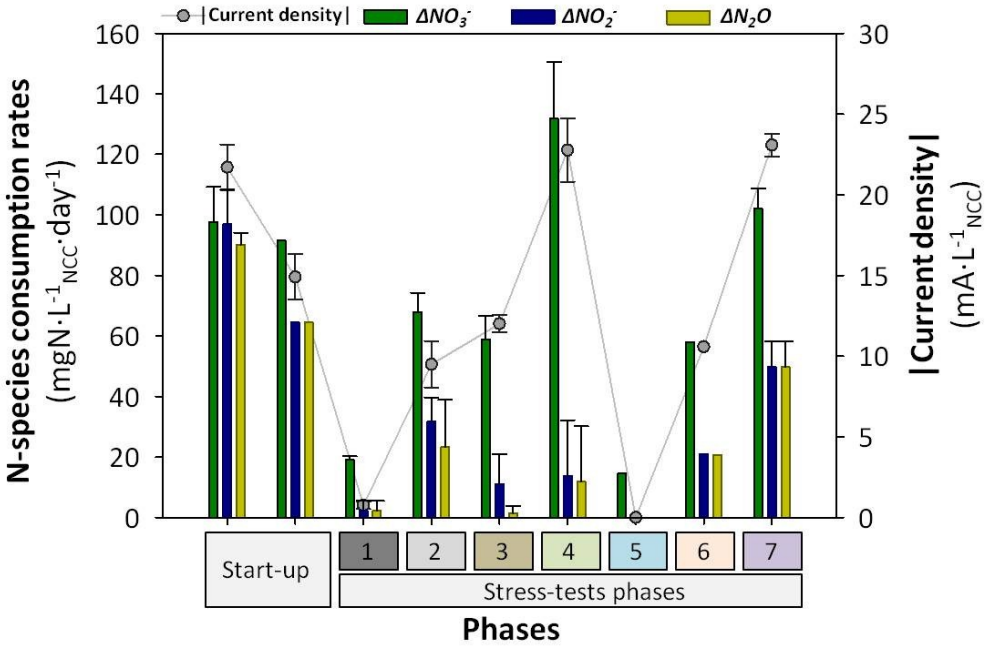

Figure S2. Current density expressed in absolute values, and nitrate, nitrite and nitrous oxide consumption rates at the phases. Error bars represent the standard deviation of the different stress-tests.

Table S2. Mean value and standard deviation of current density (in absolute value) and nitrate, nitrite and nitrous oxide consumption rates at the different phases.

Phases		j ($mA \cdot L^{-1}_{NCC}$)	ΔNO_3^- ($mgN \cdot L^{-1}_{NCC} \cdot day^{-1}$)	ΔNO_2^- ($mgN \cdot L^{-1}_{NCC} \cdot day^{-1}$)	ΔN_2O ($mgN \cdot L^{-1}_{NCC} \cdot day^{-1}$)
Start-up		21.7±1.4	97.7±11.5	96.9±11.4	90.1±4.0
		14.9±1.4	91.5±0.0	64.4±0.0	64.4±0.0
Stress-tests	**ST-1**	0.8±0.2	19.0±1.3	2.3±3.2	2.3±3.2
	ST-2	9.5±1.4	68.0±6.2	31.7±8.0	23.2±15.6
	ST-3	12.0±0.6	58.9±7.8	11.1±9.7	1.5±2.1
	ST-4	22.8±2.0	131.9±18.6	13.9±18.2	12.0±18.2
	ST-5	0.0±0.0	14.5±0.0	0.0±0.0	0.0±0.0
	ST-6	10.6±0.0	58.0±0	20.9±0.0	20.6±0.0
	ST-7	23.1±0.7	102.0±6.6	49.8±8.4	49.6±8.6

S5: Cell abundance of each gate during the whole experimental study at the different SP.

Table S3. Cell abundance of each gate at SP-A at each sampling day.

Day	G1_A	G2_A	G3_A	G4_A	G5_A	G6_A	G7_A	G8_A	G9_A	G10_A	G11_A	G12_A	G13_A	G14_A	G15_A	G16_A	G17_A	G18_A	G19_A	G20_A	G21_A
32	10.70	8.00	6.28	3.48	7.94	16.10	4.22	8.66	20.60	1.53	1.61	4.42	2.01	1.63	1.66	0.20	0.78	0.92	3.46	8.94	3.37
38	9.83	9.19	2.17	2.81	5.45	16.70	2.44	9.22	24.50	1.16	1.38	5.91	1.29	1.68	1.17	0.40	3.15	0.78	3.27	11.90	2.89
42	7.72	13.90	5.64	3.45	4.34	15.30	5.31	7.69	19.50	1.34	1.68	5.11	2.45	1.55	2.46	0.45	1.71	1.57	3.46	7.80	3.84
46	9.23	12.10	6.42	4.78	6.16	9.32	5.23	6.17	11.60	1.59	2.40	3.70	2.77	1.96	2.78	0.58	1.64	1.92	5.57	6.88	4.83
49	7.43	15.40	5.80	4.98	4.80	8.28	5.44	6.47	11.30	4.23	4.50	2.69	2.06	3.99	1.86	0.65	1.39	1.51	7.83	6.31	3.99
53	8.75	11.70	3.06	2.43	4.86	15.70	2.69	7.60	20.20	1.50	1.55	7.73	1.10	2.62	0.98	0.32	1.99	0.85	3.75	8.03	2.27
56	10.00	12.10	4.70	2.13	8.41	9.79	3.92	6.30	12.50	1.08	1.19	3.48	1.10	2.39	1.41	0.80	2.03	1.39	3.13	9.14	2.68
60	7.26	12.60	4.20	2.63	5.17	16.10	3.96	7.46	21.00	1.28	1.22	5.44	1.37	2.34	1.38	0.25	1.39	1.12	4.40	9.63	2.88
63	7.87	18.30	5.38	2.46	5.13	16.90	3.07	5.52	18.90	1.17	1.46	4.81	1.21	2.27	1.25	0.50	2.11	1.86	3.66	7.01	2.59
67	7.82	9.32	4.74	2.17	2.99	17.50	3.10	4.65	18.20	1.74	1.54	12.20	1.29	3.53	0.98	0.70	6.23	3.08	3.67	5.45	2.35
70	8.16	26.80	8.43	2.72	4.82	12.90	5.10	5.35	15.20	0.81	1.34	2.00	2.38	0.89	2.31	0.50	2.25	4.23	2.78	4.04	3.51
74	3.08	10.10	2.44	1.36	1.42	5.83	1.32	1.83	6.76	1.90	1.68	36.90	0.61	24.80	0.65	0.33	1.25	1.43	6.49	1.80	0.91
77	4.95	26.10	4.31	2.28	3.18	9.44	2.31	4.93	14.40	2.88	5.31	2.22	0.92	3.51	1.16	1.36	2.29	2.65	7.54	7.97	1.80
82	4.99	22.50	3.65	2.30	3.22	12.40	2.66	5.69	15.50	1.87	1.31	14.40	1.21	4.01	1.08	0.58	1.57	1.45	3.60	4.34	2.33
84	3.93	19.00	2.84	2.70	2.83	16.40	2.33	5.00	17.10	3.14	1.70	12.50	1.15	4.56	0.94	0.64	1.53	1.17	4.97	4.83	2.26
88	4.19	27.30	3.42	3.45	4.19	12.00	2.57	6.40	15.20	1.29	1.54	4.84	1.33	2.08	1.35	1.02	1.21	1.44	4.68	5.85	3.25
95	4.05	25.20	3.48	2.97	3.91	10.90	3.70	4.93	11.20	1.35	2.84	3.72	3.37	1.96	1.82	0.39	0.60	2.07	5.17	4.70	3.30
97	3.18	31.60	2.41	2.53	3.93	15.10	2.46	3.71	14.30	1.65	2.31	6.16	2.11	2.60	1.30	0.50	0.51	1.31	4.68	3.77	2.39
102	2.17	13.30	1.43	34.60	2.43	8.15	2.12	2.46	7.35	21.00	4.48	2.37	0.99	1.03	0.79	0.11	0.17	0.60	23.70	2.59	14.30
104	3.38	27.90	2.48	2.57	4.50	11.90	2.41	4.66	13.50	1.04	1.81	4.35	1.93	1.96	1.33	0.22	0.56	1.11	4.27	6.36	2.62

Table S4. Cell abundance of each gate at SP-B at each sampling day.

Day	G1_B	G2_B	G3_B	G4_B	G5_B	G6_B	G7_B	G8_B	G9_B	G10_B	G11_B	G12_B	G13_B	G14_B	G15_B	G16_B	G17_B	G18_B	G19_B	G20_B	G21_B
32	2.74	8.18	2.42	1.75	3.70	13.40	2.34	7.11	14.40	1.51	1.75	8.05	0.84	3.09	0.66	0.07	0.25	0.99	3.01	13.70	1.69
38	5.48	8.38	2.39	2.11	4.56	15.20	2.36	6.01	16.10	1.39	1.47	8.48	0.98	2.90	0.98	0.21	1.35	0.76	3.09	10.10	2.24
42	7.51	10.10	3.61	2.83	6.05	13.00	3.71	6.88	16.30	1.39	1.51	6.97	1.73	2.28	1.60	0.27	1.43	0.88	3.18	9.36	3.46
46	9.51	12.50	5.77	3.64	7.34	10.10	5.19	6.53	12.60	1.42	1.63	4.20	2.04	1.92	2.52	0.43	1.57	1.51	4.16	8.17	4.40
49	8.97	11.10	6.80	5.00	5.24	7.58	6.73	5.67	9.02	4.10	4.08	3.43	2.65	5.44	2.22	0.71	1.90	1.80	7.97	6.31	4.33
53	3.74	10.30	2.52	1.82	5.22	14.80	5.01	5.85	15.20	1.35	1.18	8.90	4.78	2.68	1.54	0.86	0.48	0.79	2.80	9.95	3.82
56	6.21	14.10	3.95	2.33	6.29	13.30	4.49	5.47	14.40	1.48	1.41	6.81	1.83	2.91	1.39	1.55	1.11	1.49	3.37	7.62	3.32
60	8.11	17.20	4.98	2.02	5.98	12.40	3.66	6.65	15.10	1.24	1.00	5.44	1.11	2.50	1.27	1.86	1.75	1.75	2.99	7.63	2.26
63	7.07	16.10	4.69	2.06	5.31	16.00	3.00	4.97	16.20	1.24	1.28	7.05	1.17	2.50	1.16	3.44	1.96	1.98	3.02	6.90	2.30
67	7.06	10.20	6.35	2.15	4.35	11.60	4.58	6.14	12.30	1.33	1.44	6.41	1.85	2.52	1.46	2.68	5.85	4.29	3.05	6.88	2.67
70	5.90	21.30	5.75	1.99	4.56	15.60	3.81	5.23	16.90	1.21	1.50	6.35	1.72	2.70	1.57	2.43	1.55	2.89	2.99	5.38	2.44
74	4.40	23.40	4.18	1.88	3.98	15.90	3.60	5.58	18.60	1.11	1.21	5.80	2.19	2.36	1.41	2.97	1.83	2.27	2.80	6.17	2.62
77	3.21	17.80	2.47	1.86	3.81	16.20	2.19	6.15	18.40	2.22	3.38	7.43	0.99	3.64	0.87	5.08	1.09	1.43	5.41	7.84	1.63
82	3.53	16.20	2.55	2.02	4.27	15.80	3.74	6.19	16.40	1.42	1.40	10.20	3.28	3.89	1.47	3.41	0.87	1.19	3.51	6.37	3.24
84	3.35	18.60	2.54	2.06	3.88	15.80	2.77	6.85	16.50	1.39	1.44	9.75	1.82	3.63	1.09	2.75	1.29	1.24	3.37	6.77	2.62
88	4.07	30.50	3.60	3.05	4.03	10.90	2.48	6.09	14.50	1.17	1.45	4.33	1.20	2.12	1.29	0.76	1.35	1.61	4.30	5.55	3.03
95	3.88	19.30	3.06	2.63	5.55	12.20	2.93	8.31	15.90	1.03	1.51	4.64	1.83	1.92	1.55	0.49	0.55	1.30	3.92	9.02	2.82
97	2.63	22.00	2.01	2.60	3.86	16.30	2.53	6.67	19.00	1.28	1.52	7.79	1.57	2.64	1.05	0.69	0.51	0.82	4.11	7.73	2.72
102	2.96	19.70	1.76	2.10	4.21	13.80	1.85	8.76	18.10	0.95	1.10	8.46	1.04	1.96	1.06	0.51	0.35	0.69	3.25	9.61	2.03
104	2.74	20.30	1.93	2.92	4.19	12.50	2.01	8.90	18.30	0.95	1.21	4.60	1.25	1.90	1.13	0.38	0.59	0.68	3.93	10.00	2.91

Table S5. Cell abundance of each gate at SP-C at each sampling day.

Day	G1_C	G2_C	G3_C	G4_C	G5_C	G6_C	G7_C	G8_C	G9_C	G10_C	G11_C	G12_C	G13_C	G14_C	G15_C	G16_C	G17_C	G18_C	G19_C	G20_C	G21_C
32	6.40	11.30	6.85	3.26	3.70	22.80	4.76	7.00	29.30	1.29	1.47	3.64	1.86	1.52	2.05	0.26	0.77	2.18	3.53	7.95	3.23
38	6.36	11.50	5.39	3.01	4.08	24.30	4.19	7.40	31.70	1.28	1.37	3.93	1.58	1.58	1.67	0.18	1.15	1.51	3.35	8.22	3.21
42	8.38	11.50	5.71	3.85	4.34	20.30	4.17	6.26	23.40	1.52	1.75	4.18	1.76	2.24	1.89	0.21	1.90	1.51	4.56	7.97	3.75
46	7.48	10.40	6.08	3.11	5.06	14.70	4.48	7.95	18.50	1.29	1.60	3.96	1.68	1.93	2.16	0.33	1.15	1.57	3.85	9.72	3.57
49	7.90	11.70	6.20	5.30	4.83	8.17	5.80	5.68	10.30	4.88	4.63	3.21	1.94	5.67	1.91	0.41	1.35	1.55	8.56	6.80	4.09
53	5.09	9.59	2.10	2.09	5.47	11.10	2.20	9.50	15.10	1.05	1.17	4.38	0.62	2.05	0.84	0.39	0.50	0.42	2.71	13.80	2.14
56	9.54	11.00	6.17	2.78	8.11	10.20	4.70	7.34	13.40	0.97	1.26	3.25	1.27	1.86	1.86	0.46	1.24	1.55	3.02	10.20	3.60
60	7.28	10.60	8.85	2.57	4.05	13.90	6.20	7.29	17.40	1.23	1.35	5.47	2.28	2.40	2.48	0.28	1.13	2.56	3.39	8.58	3.62
63	6.37	11.90	7.74	2.46	7.47	11.70	4.27	7.07	14.00	1.01	1.31	3.97	1.22	2.09	1.86	0.49	1.29	4.45	3.16	9.06	3.19
67	6.17	8.51	6.62	4.68	3.60	14.80	4.24	5.33	15.20	1.10	3.04	4.37	1.44	3.14	1.44	0.68	7.49	4.35	9.64	6.45	3.13
70	6.68	21.60	7.89	2.61	4.81	17.90	4.91	5.10	19.40	0.80	1.64	3.05	1.96	1.27	2.07	0.63	2.32	4.39	3.54	4.55	3.07
74	6.26	24.10	5.84	7.43	3.13	9.88	2.72	3.91	13.30	8.48	6.95	1.91	1.23	1.19	1.25	0.60	3.14	3.35	11.30	4.05	2.74
77	6.23	10.30	3.90	2.92	8.33	8.48	2.93	5.83	11.70	1.18	1.15	2.99	0.91	1.48	1.18	0.94	0.78	1.43	3.15	9.55	3.53
82	6.78	26.30	5.32	2.79	4.96	11.90	3.57	6.82	16.40	0.99	1.43	3.33	1.53	1.56	1.59	0.65	2.55	2.43	3.53	5.58	3.24
84	6.16	27.50	5.38	2.78	4.47	10.60	3.77	6.01	13.90	1.04	1.44	3.57	1.58	1.80	1.58	0.59	3.25	2.72	3.70	4.89	3.19
88	4.40	22.90	3.56	3.24	4.58	13.40	3.33	5.99	16.10	1.20	1.56	5.94	1.85	2.24	1.59	0.92	1.06	1.56	4.74	6.27	3.54
95	4.88	21.50	3.98	3.32	6.34	10.80	3.91	5.46	12.50	1.13	2.25	3.62	2.77	1.74	2.08	0.37	0.59	2.11	4.90	6.42	3.97
97	3.50	14.90	2.88	4.72	6.86	12.90	3.03	6.60	16.00	1.64	1.91	5.76	1.18	2.24	1.22	0.58	0.48	0.98	5.45	8.84	4.32
102	4.22	25.20	2.95	3.14	5.77	11.80	2.59	5.51	15.20	1.11	1.69	3.83	1.65	1.86	1.47	0.41	0.37	1.43	4.29	7.51	3.46
104	3.54	15.10	3.94	4.75	6.47	11.70	4.22	5.98	14.60	1.46	1.78	4.42	1.42	1.88	1.21	0.47	0.55	1.02	5.32	8.47	4.50

Table S6. Cell abundance of each gate at SP-D at each sampling day.

Day	G1_D	G2_D	G3_D	G4_D	G5_D	G6_D	G7_D	G8_D	G9_D	G10_D	G11_D	G12_D	G13_D	G14_D	G15_D	G16_D	G17_D	G18_D	G19_D	G20_D	G21_D
38	5.41	8.54	3.15	22.10	2.19	10.00	4.50	3.16	11.10	13.40	0.93	1.47	1.01	0.67	0.92	0.33	1.87	0.93	8.87	19.10	14.60
42	16.90	15.50	9.50	3.60	6.70	11.00	5.88	5.30	14.50	1.19	2.05	2.23	3.12	1.08	2.66	0.40	2.85	1.83	3.41	4.95	4.36
46	10.00	14.00	5.77	5.18	6.02	9.00	4.33	5.91	12.20	1.87	2.83	3.56	2.54	2.03	2.29	0.71	1.78	1.25	6.01	6.39	4.73
49	12.30	13.90	5.26	4.48	6.86	7.23	5.00	6.55	10.60	1.82	2.59	2.91	2.03	2.11	1.74	0.83	2.22	1.36	5.44	6.45	4.24
53	12.70	12.50	6.27	3.08	6.21	8.93	4.40	6.05	11.00	1.53	1.90	4.17	1.59	2.19	1.75	0.67	2.87	1.90	4.18	6.48	3.01
56	13.30	14.20	7.15	2.83	6.84	9.21	5.03	4.75	11.40	1.39	1.93	3.45	1.62	2.10	1.92	0.76	2.59	2.06	4.02	6.35	3.04
60	11.30	18.30	5.97	3.27	6.08	9.02	4.48	5.68	12.10	1.72	1.83	2.71	1.54	1.75	1.91	0.47	2.50	1.73	4.51	5.36	3.03
63	9.74	14.50	6.85	2.51	5.69	11.50	3.75	5.22	12.30	1.54	1.85	4.41	1.71	2.09	1.76	0.58	2.08	2.46	4.01	5.82	2.70
67	26.40	9.91	8.49	16.20	8.94	5.17	2.57	2.21	5.65	12.10	3.09	1.77	0.81	0.82	1.05	0.23	6.02	1.90	9.98	1.73	5.99
70	10.80	25.50	11.30	2.51	4.54	11.40	5.70	4.91	13.40	0.96	1.77	1.53	2.31	0.98	2.30	0.51	2.37	4.41	2.93	3.53	3.18
74	9.14	33.20	6.66	1.99	4.25	10.40	3.20	4.23	13.50	0.80	1.59	1.65	1.45	1.52	1.42	0.86	3.90	3.04	2.94	3.93	2.26
77	7.10	30.80	3.44	1.67	3.55	10.80	1.94	3.90	14.80	1.13	2.82	2.25	0.99	2.74	0.90	1.54	2.96	1.72	4.52	7.15	1.58
82	32.10	16.70	14.50	2.32	11.10	7.84	3.29	3.47	10.20	0.81	1.87	1.83	1.36	1.24	1.46	0.44	4.88	2.49	3.61	2.61	2.61
84	6.56	29.40	4.56	2.73	4.10	10.40	3.00	5.72	13.80	1.18	1.74	3.11	1.33	1.60	1.20	0.78	3.33	1.98	3.68	4.35	2.68
88	4.46	27.70	2.98	3.56	4.20	11.80	2.26	4.97	14.10	1.57	2.07	4.75	1.28	2.64	1.07	1.31	1.42	1.23	5.23	4.94	3.08
95	4.31	21.40	2.89	4.26	4.04	11.40	2.96	6.77	14.70	1.77	2.92	4.03	2.14	2.44	1.34	0.47	0.73	1.11	6.49	5.38	3.66
97	3.80	33.30	2.56	2.59	4.18	14.80	2.34	3.44	14.30	1.54	2.41	5.50	1.98	2.34	1.14	0.46	0.74	1.29	4.64	3.03	2.39
102	2.17	21.10	1.44	20.30	2.66	7.06	1.74	2.47	8.58	20.90	7.13	1.80	1.09	1.90	0.63	0.15	0.27	0.71	21.70	2.28	6.10

S6: Box plot for cell abundances of each gate during the whole experimental study.

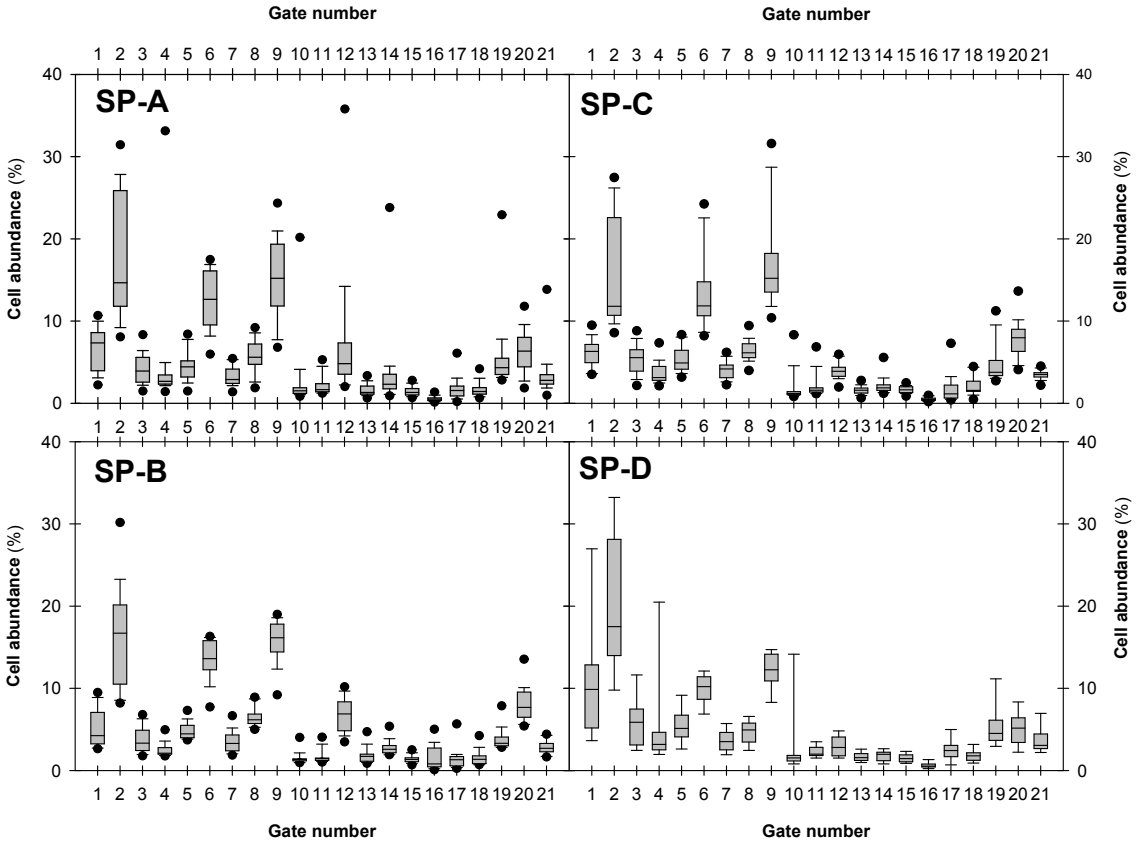

Figure S3. The box plot shows the relative cell abundance of each gate (numbered as gate number) at each sampling port (SP-A, –B, -C and –D) during the whole experimental study. The box plot allows an easy visualization of which gates are the most abundant at each sampling port. In this study, gates 2, 6 and 9 were the most abundant in sampling ports SP-A, -B and -C, while gates 1, 2, 6 and 9 were the most abundant in sampling port SP-D.

S7: Correlation data between gate cell abundances and reactor performance using data of ST-4 and ST-5 phases.

Table S7. Correlation of SP-A gates with reactor performance using data of ST-4 and ST-5 phases. The different gates have been labeled as G*X*_*Y*, where: *X* = gate number and *Y* = sampling port. Reactor performance data included: pH at cathode effluent (pHeff), current density (Current_den), coulombic efficiency (*CE*) and nitrate, nitrite and nitrous oxide consumption rates (ΔNO_3^-, ΔNO_2^- and ΔN_2O, respectively). Green colored indicates positive correlations higher than 0.4.

	Current_den	ΔNO_3^-	ΔNO_2^-	ΔN_2O	***CE***
Current_den	1.0	0.9	0.1	0.2	0.9
ΔNO_3^-	0.9	1.0	0.4	0.4	0.7
ΔNO_2^-	0.1	0.4	1.0	0.9	-0.2
ΔN_2O	0.2	0.4	0.9	1.0	-0.2
CE	0.9	0.7	-0.2	-0.2	1.0
pHeff	0.7	0.5	0.1	0.2	0.4
G1_A	-0.4	-0.4	-0.5	-0.5	-0.3
G2_A	0.5	0.7	0.6	0.6	0.3
G3_A	-0.2	-0.1	-0.4	-0.4	0.0
G4_A	0.3	0.3	0.0	0.0	0.2
G5_A	0.3	0.4	0.0	0.0	0.2
G6_A	-0.1	-0.1	-0.2	0.0	-0.3
G7_A	0.0	0.0	-0.3	-0.2	0.0
G8_A	0.2	0.2	-0.2	-0.3	0.1
G9_A	-0.1	-0.1	-0.2	-0.2	-0.3
G10_A	-0.1	-0.1	0.2	0.0	-0.2
G11_A	-0.3	0.0	0.6	0.3	-0.3
G12_A	0.0	-0.2	-0.2	-0.2	0.1
G13_A	0.2	0.3	0.2	0.4	0.0
G14_A	0.0	-0.2	-0.1	-0.1	0.2
G15_A	0.2	0.3	0.0	0.0	0.2
G16_A	-0.3	-0.1	0.3	0.0	-0.3
G17_A	-0.9	-0.9	-0.4	-0.4	-0.8
G18_A	-0.5	-0.4	-0.3	-0.3	-0.3
G19_A	-0.1	0.0	0.4	0.2	-0.1
G20_A	-0.3	-0.1	0.0	-0.2	-0.3
G21_A	0.2	0.2	-0.2	-0.1	0.2

Table S8. Correlation of SP-B gates with reactor performance using data of ST-4 and ST-5 phases. The different gates have been labeled as G*X*_*Y*, where: *X* = gate number and *Y* = sampling port. Reactor performance data included: pH at cathode effluent (pHeff), current density (Current_den), coulombic efficiency (*CE*) and nitrate, nitrite and nitrous oxide consumption rates (ΔNO_3^-, ΔNO_2^- and ΔN_2O, respectively). Green colored indicates positive correlations higher than 0.4.

	Current_den	ΔNO_3^-	ΔNO_2^-	ΔN_2O	***CE***
Current_den	1.0	0.9	0.1	0.2	0.9
ΔNO_3^-	0.9	1.0	0.4	0.4	0.7
ΔNO_2^-	0.1	0.4	1.0	0.9	-0.2
ΔN_2O	0.2	0.4	0.9	1.0	-0.2
CE	0.9	0.7	-0.2	-0.2	1.0
pHeff	0.7	0.5	0.1	0.2	0.4
G1_B	-0.5	-0.6	-0.7	-0.6	-0.2
G2_B	0.6	0.5	0.1	0.3	0.6
G3_B	-0.5	-0.7	-0.7	-0.6	-0.3
G4_B	0.2	0.2	0.2	0.4	0.1
G5_B	0.0	0.0	-0.5	-0.4	0.2
G6_B	0.4	0.5	0.3	0.3	0.3
G7_B	-0.5	-0.6	-0.5	-0.5	-0.3
G8_B	0.0	0.0	0.5	0.5	-0.3
G9_B	0.5	0.6	0.6	0.5	0.4
G10_B	-0.3	0.0	0.4	0.1	-0.4
G11_B	-0.3	0.0	0.5	0.2	-0.3
G12_B	0.3	0.3	0.2	0.1	0.0
G13_B	0.2	0.1	-0.1	-0.2	0.1
G14_B	0.1	0.3	0.2	-0.1	0.0
G15_B	-0.1	-0.2	-0.6	-0.5	0.1
G16_B	-0.3	-0.2	-0.1	-0.4	-0.2
G17_B	-0.9	-0.9	-0.5	-0.4	-0.7
G18_B	-0.8	-0.9	-0.6	-0.5	-0.5
G19_B	0.0	0.2	0.7	0.4	-0.2
G20_B	-0.3	0.0	0.7	0.5	-0.5
G21_B	0.4	0.2	-0.1	0.0	0.2

Table S9. Correlation of SP-C gates with reactor performance using data of ST-4 and ST-5 phases. The different gates have been labeled as G*X*_*Y*, where: *X* = gate number and *Y* = sampling port. Reactor performance data included: pH at cathode effluent (pHeff), current density (Current_den), coulombic efficiency (*CE*) and nitrate, nitrite and nitrous oxide consumption rates (ΔNO_3^-, ΔNO_2^- and ΔN_2O, respectively). Green colored indicates positive correlations higher than 0.4.

	Current_den	ΔNO_3^-	ΔNO_2^-	ΔN_2O	***CE***
Current_den	1.0	0.9	0.1	0.2	0.9
ΔNO_3^-	0.9	1.0	0.4	0.4	0.7
ΔNO_2^-	0.1	0.4	1.0	0.9	-0.2
ΔN_2O	0.2	0.4	0.9	1.0	-0.2
CE	0.9	0.7	-0.2	-0.2	1.0
pHeff	0.7	0.5	0.1	0.2	0.4
G1_C	-0.2	-0.3	-0.6	-0.8	0.1
G2_C	0.7	0.5	-0.2	-0.2	0.7
G3_C	-0.2	-0.3	-0.8	-0.7	0.1
G4_C	-0.3	-0.4	0.1	0.2	-0.2
G5_C	0.1	0.4	0.6	0.4	-0.1
G6_C	-0.1	-0.2	-0.3	-0.1	-0.1
G7_C	-0.1	-0.2	-0.6	-0.5	0.0
G8_C	0.4	0.5	0.3	0.3	0.1
G9_C	0.3	0.2	-0.1	0.0	0.2
G10_C	0.0	-0.1	-0.1	0.0	0.2
G11_C	-0.2	-0.4	-0.2	-0.1	0.0
G12_C	0.1	0.1	0.3	0.5	-0.2
G13_C	0.3	0.1	-0.5	-0.4	0.4
G14_C	-0.5	-0.5	0.0	0.1	-0.7
G15_C	0.3	0.2	-0.6	-0.6	0.5
G16_C	-0.3	-0.1	0.2	0.0	-0.2
G17_C	-0.7	-0.9	-0.5	-0.5	-0.6
G18_C	-0.3	-0.5	-0.8	-0.7	0.0
G19_C	-0.5	-0.6	-0.2	0.0	-0.4
G20_C	-0.2	0.1	0.6	0.5	-0.4
G21_C	0.2	0.4	0.8	0.9	-0.2

S8: Correlation data between gate cell abundances and reactor performance using the whole dataset.

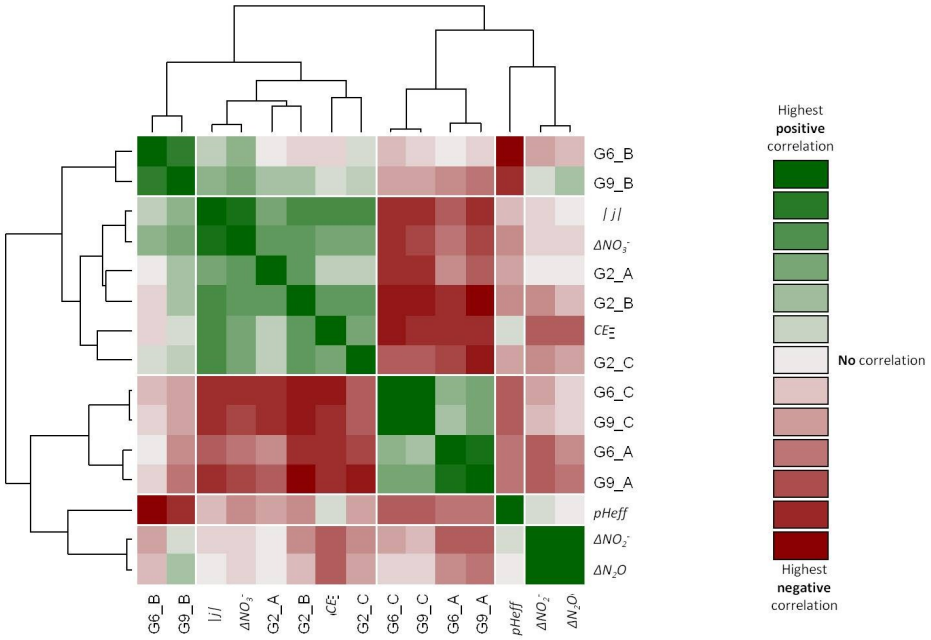

Figure S4. Correlation of the most abundant subcommunities G2, G6 and G9 with reactor performance using Spearman's rank correlation in the whole monitored period. Strong positive correlation is indicated by color red. Strong negative correlation is indicated by blue. The different gates have been labeled as G*X*_*Y*, where: *X* = gate number and *Y* = sampling port. Reactor performance included: pH at cathode effluent (*pHeff*), absolute current density (|*j*|), coulombic efficiency (*CE*) and nitrate, nitrite and nitrous oxide consumption rates (ΔNO_3^-, ΔNO_2^- and ΔN_2O, respectively).

Table S10. Correlation of SP-A gates with reactor performance using the whole dataset. The different gates have been labeled as G*X*_*Y*, where: *X* = gate number and *Y* = sampling port. Reactor performance data included: pH at cathode effluent (pHeff), current density (Current_den), coulombic efficiency (*CE*) and nitrate, nitrite and nitrous oxide consumption rates (ΔNO_3^-, ΔNO_2^- and ΔN_2O, respectively). Green colored indicates positive correlations higher than 0.4.

	Current_den	ΔNO_3^-	ΔNO_2^-	ΔN_2O	***CE***
Current_den	1.0	0.9	0.2	0.2	0.8
ΔNO_3^-	0.9	1.0	0.2	0.2	0.6
ΔNO_2^-	0.2	0.2	1.0	0.9	-0.2
ΔN_2O	0.2	0.2	0.9	1.0	-0.2
CE	0.8	0.6	-0.2	-0.2	1.0
pHeff	0.1	0.0	0.3	0.2	0.3
G1_A	-0.7	-0.6	-0.3	-0.4	-0.4
G2_A	0.6	0.7	0.2	0.2	0.4
G3_A	-0.3	-0.2	-0.5	-0.6	-0.1
G4_A	0.2	0.1	0.4	0.5	0.0
G5_A	-0.4	-0.4	-0.2	-0.2	-0.1
G6_A	-0.2	-0.2	-0.2	-0.1	-0.3
G7_A	-0.4	-0.4	-0.2	-0.2	-0.1
G8_A	-0.5	-0.4	-0.1	-0.2	-0.3
G9_A	-0.4	-0.3	-0.2	-0.2	-0.4
G10_A	0.2	0.1	0.4	0.4	0.0
G11_A	0.0	0.1	0.5	0.3	-0.2
G12_A	0.1	0.1	-0.3	-0.2	0.1
G13_A	-0.2	-0.2	0.1	0.1	-0.1
G14_A	0.1	0.1	-0.2	-0.2	0.2
G15_A	-0.2	-0.2	0.0	-0.1	0.0
G16_A	0.0	0.2	-0.1	-0.3	-0.1
G17_A	-0.5	-0.4	-0.3	-0.3	-0.6
G18_A	-0.1	0.0	-0.4	-0.4	-0.1
G19_A	0.2	0.1	0.5	0.5	0.1
G20_A	-0.6	-0.5	0.0	-0.1	-0.3
G21_A	0.2	0.0	0.4	0.5	0.0

Table S11. Correlation of SP-B gates with reactor performance using the whole dataset. The different gates have been labeled as G*X_Y,* where: *X* = gate number and *Y* = sampling port. Reactor performance data included: pH at cathode effluent (pHeff), current density (Current_den), coulombic efficiency (*CE*) and nitrate, nitrite and nitrous oxide consumption rates (ΔNO_3^-, ΔNO_2^- and ΔN_2O, respectively). Green colored indicates positive correlations higher than 0.4.

	Current_den	ΔNO_3^-	ΔNO_2^-	ΔN_2O	***CE***
G1_B	-0.4	-0.4	-0.2	-0.3	0.0
G2_B	0.8	0.7	0.0	0.1	0.7
G3_B	-0.3	-0.3	-0.5	-0.5	0.0
G4_B	0.0	-0.1	0.2	0.1	0.0
G5_B	-0.3	-0.3	0.0	-0.1	0.1
G6_B	0.4	0.5	0.0	0.1	0.1
G7_B	-0.4	-0.3	-0.2	-0.4	-0.1
G8_B	0.1	-0.1	0.5	0.6	-0.1
G9_B	0.5	0.6	0.3	0.5	0.3
G10_B	-0.3	-0.1	0.0	-0.2	-0.2
G11_B	-0.2	-0.1	0.1	-0.1	-0.2
G12_B	0.1	0.3	0.1	0.1	-0.2
G13_B	-0.1	0.0	0.0	-0.2	0.0
G14_B	-0.1	0.1	-0.1	-0.3	-0.1
G15_B	-0.1	-0.1	0.0	-0.2	0.1
G16_B	0.2	0.4	-0.4	-0.5	0.2
G17_B	-0.4	-0.4	-0.4	-0.4	-0.4
G18_B	-0.2	-0.2	-0.6	-0.6	-0.1
G19_B	0.0	0.1	0.2	0.0	0.0
G20_B	-0.5	-0.5	0.3	0.3	-0.5
G21_B	-0.1	-0.1	0.1	0.0	0.0

Table S12. Correlation of SP-C gates with reactor performance using the whole dataset. The different gates have been labeled as G*X*_*Y*, where: *X* = gate number and *Y* = sampling port. Reactor performance data included: pH at cathode effluent (pHeff), current density (Current_den), coulombic efficiency (*CE*) and nitrate, nitrite and nitrous oxide consumption rates (ΔNO_3^-, ΔNO_2^- and ΔN_2O, respectively). Green colored indicates positive correlations higher than 0.4.

	Current_den	ΔNO_3^-	ΔNO_2^-	ΔN_2O	***CE***
G1_C	-0.4	-0.3	-0.3	-0.5	0.0
G2_C	0.7	0.6	-0.1	0.0	0.6
G3_C	-0.2	-0.3	-0.7	-0.6	0.2
G4_C	0.0	-0.1	0.1	0.2	-0.1
G5_C	0.3	0.3	0.4	0.2	0.2
G6_C	-0.4	-0.3	-0.1	0.1	-0.4
G7_C	-0.3	-0.4	-0.4	-0.4	0.1
G8_C	-0.3	-0.2	0.1	0.0	-0.2
G9_C	-0.4	-0.3	0.0	0.1	-0.4
G10_C	0.0	0.0	-0.1	-0.1	0.2
G11_C	0.0	-0.1	-0.1	-0.1	0.1
G12_C	0.1	0.1	0.2	0.3	-0.1
G13_C	-0.1	-0.3	-0.2	-0.1	0.2
G14_C	-0.2	-0.3	0.0	0.0	-0.2
G15_C	-0.2	-0.3	-0.4	-0.4	0.2
G16_C	0.4	0.5	-0.2	-0.2	0.2
G17_C	-0.2	-0.2	-0.5	-0.4	-0.3
G18_C	0.0	0.0	-0.7	-0.6	0.1
G19_C	-0.1	-0.2	-0.1	0.0	-0.2
G20_C	-0.3	-0.2	0.4	0.2	-0.3
G21_C	0.2	0.1	0.4	0.4	0.1

Table S13. Gates with positive correlations higher than 0.4 to reactor performance using the whole dataset. The different gates have been labeled as G*X*_*Y*, where: *X* = gate number and *Y* = sampling port. Reactor performance data included: current density (Current_den), coulombic efficiency (*CE*) and nitrate, nitrite and nitrous oxide consumption rates (ΔNO_3^-, ΔNO_2^- and ΔN_2O, respectively).

Current_den		ΔNO_3^-		ΔNO_2^-		ΔN_2O		***CE***	
G2_A	0.6	**G2_A**	0.7	**G4_A**	0.4	**G4_A**	0.5	**G2_A**	0.4
G2_B	0.8	**G2_B**	0.7	**G10_A**	0.4	**G10_A**	0.4	**G2_B**	0.7
G6_B	0.4	**G6_B**	0.5	**G11_A**	0.5	**G19_A**	0.5	**G2_C**	0.6
G9_B	0.5	**G9_B**	0.6	**G19_A**	0.5	**G21_A**	0.5		
G2_C	0.7	**G16_B**	0.4	**G21_A**	0.4	**G8_B**	0.6		
G16_C	0.4	**G2_C**	0.6	**G8_B**	0.5	**G9_B**	0.5		
		G16_C	0.5	**G5_C**	0.4	**G21_C**	0.4		
				G20_C	0.4				
				G21_C	0.4				

S9: Dynamics on G2 cell abundance organized through nitrate consumption rate.

Table S14. G2 cell abundance dynamics at SP-A, SP-B and SP-C organized through nitrate consumption rate. Other parameters of reactor performance are also shown organized through nitrate consumption rate.

ΔNO_3^-	G2 cell abundance (%)			Sampling day	Current density	ΔNO_2^-	ΔN_2O
($mgN \cdot L^{-1}_{NCC} \cdot d^{-1}$)	SP-A	SP-B	SP-C	(day)	($mA \cdot L^{-1}_{NCC}$)	($mgN \cdot L^{-1}_{NCC} \cdot d^{-1}$)	($mgN \cdot L^{-1}_{NCC} \cdot d^{-1}$)
14.5	9.32	10.20	8.51	67	0.00	0.0	0.0
19.9	8.00	8.18	11.30	32	0.59	0.0	0.0
53.4	12.60	17.20	10.60	60	11.61	4.2	0.0
58.0	25.20	19.30	21.50	95	10.58	20.9	20.6
62.8	9.19	8.38	11.50	38	7.77	41.4	41.4
64.4	12.10	14.10	11.00	56	12.40	18.0	3.0
65.4	11.70	10.30	9.59	53	8.06	29.3	15.6
65.8	15.40	11.10	11.70	49	10.45	24.5	9.8
67.1	12.10	12.50	10.40	46	10.64	24.5	10.4
78.8	13.90	10.10	11.50	42	10.53	38.7	38.7
97.3	27.90	20.30	15.10	104	22.58	43.8	43.6
99.5	10.10	23.40	24.10	74	19.17	6.0	6.0
106.7	13.30	19.70	25.20	102	23.56	55.7	55.7
109.8	26.10	17.80	10.30	77	11.90	33.9	14.1
122.4	19.00	18.60	27.50	84	25.02	0.0	0.0
124.2	26.80	21.30	21.60	70	21.47	0.0	0.0
128.7	27.30	30.50	22.90	88	23.31	8.3	8.0
132.2	18.30	16.10	11.90	63	22.01	0.0	0.0
155.5	31.60	22.00	14.90	97	23.80	52.7	52.2
157.1	22.50	16.20	26.30	82	25.04	19.0	5.0

S10: Contribution of *Thiobacillus* sp. according to T-RFLP analysis of the samples taken directly from the cathode volume.

Table S15. Contribution of the terminal restriction fragment affiliated to *Thiobacillus* sp. in the complete community based on T-RFLP. Data shown in percentage (%).

Stress-test	Day	SP-A	SP-B	SP-C
ST-1	**31**	0	0	0
ST-2	**45**	23	6	4
ST-3	**59**	15	23	10
ST-4	**62**	15	19	11
ST-5	**66**	5	3	2
ST-4	**69**	26	23	12
ST-4	**83**	30	33	25
ST-6	**95**	30	10	15
ST-7	**104**	54	10	14

References

(1) Thieme Chemistry (Hrsg.): *RÖMPP Online - Version 3.5*. Georg Thieme Verlag KG. Stuttgart **2009**.

(2) Ansys. Ansys fluent theory guide. Inc Northbrook IL**. 2009**. 49–53.